JOURNAL OF MATERIALS SCIENCE 9 (1974) 1847–1854

Interfacial bonding and the toughness of carbon fibre reinforced glass and glass-ceramics

D. C. PHILLIPS

Process Technology Division, UKAEA Research Group, Atomic Energy Research Establishment, Harwell, Oxon, UK

The work of fracture of four different carbon fibre reinforced glass and glass-ceramic composites has been measured to determine the effects of the different properties of the components on fracture behaviour. Differences in fracture energies can be explained in terms of the fibre pull-out model and differences in the fibre-matrix interfacial shear bond. The work of fracture of the glass-ceramic is independent of crack velocity while that of the Pyrex matrix composite decreases with increasing velocity at low velocities, the decrease stopping at higher velocities. Work of fracture values agree well with linear elastic fracture mechanics toughness values.

1. Introduction

The main inhibition in the use of ceramics for structural components is their brittleness, or low fracture surface energy. In many technologies, and in particular in the development of gas turbine engines, it is desirable to develop tough materials which are capable of withstanding higher temperatures and more corrosive environments than metals. Ceramics are in many ways suitable, but their brittleness renders them susceptible to failure under conditions of thermal or mechanical shock. One way of increasing the fracture surface energy, and thus decreasing the brittleness, of ceramics is to incorporate within them fibres to produce a composite material. A suitable system for studying the mechanical behaviour of brittle fibre reinforced ceramics is carbon fibre reinforced glass and several papers have described the fabrication and mechanical properties of this and related systems [1-4].

This paper presents the results of some measurements which have been carried out on several different carbon fibre reinforced glass (CFRG) and glass-ceramic (CFRGC) systems in order to investigate how varied fibre and matrix properties affect the fracture behaviour of the composite. The materials consisted of high modulus and high strength carbon fibres in matrices of Pyrex glass and a lithium alumino-silicate glass-ceramic. Fracture energies have been determined by the work of fracture technique using circumferentially notched bars in which the continuous, aligned fibres were parallel to the bar axes and crack propagation was perpendicular to the fibre direction. Earlier work on Pyrex glass reinforced with high modulus carbon fibre has shown that high fracture energies are obtained in this mode, due to the large amounts of work necessary to extract broken fibres from the matrix against restraining interfacial shear stresses [5].

The work of fracture values [6] (γ_F) of homogeneous, isotropic ceramics agree well with fracture toughness values (G_{1C}) obtained by linear elastic fracture mechanics (LEFM) techniques, provided the work of fracture is measured under well controlled fracture conditions [7]. (Because of the difference in the conventional definitions of work of fracture and fracture toughness, $\phi G_{1C} = 2\gamma_F$.) It is not clear *a priori* that this should also be true for fibre reinforced ceramics as it is arguable that the fibre pull-out process results in a contribution to energy absorption from work done after the onset of fracture, during the separation of the fracture surfaces. Where the work of fracture is dominated by the fibre pull-out process, the work of fracture may not be appropriate to the

onset of fracture, which is instead determined by other mechanisms leading to a smaller energy absorption corresponding to the LEFM toughness. Approximate measurements of G_{1C} were obtained in earlier work and compared with γ_F values. More accurate measurements are reported here, precautions having been taken to ensure that cracks propagate in the correct direction perpendicular to fibres, without deflecting into low energy directions parallel to fibres.

2. Experimental

The materials all contained continuous, aligned 8 μm diameter, carbon fibres and were manufactured by a hot-pressing process. The glass-ceramic was a low expansion lithium aluminosilicate supplied by English Electric (NK2-1106). Table I describes properties of some of the fibres and matrices and Table II describes the properties of four composites (P1, P2, GC1 and GC2). In Table I the flexural strength and modulus of the glass and glass-ceramic are values obtained from measurements on unreinforced materials. The tensile strengths and Young's moduli of the fibres were obtained directly from measurements of the fibres used to make these composites. The compositions of the materials in Table II were determined by density and burn-out measurements. Bend and interlaminar shear strengths were measured by three-point bend tests on rectangular bars of 2.5 mm width, 1.0 mm thickness and 30 and 4 mm spans respectively. Some measurements were also carried out on two other composites, P3 and P4. Like P1, these consisted of Pyrex glass reinforced with high modulus carbon fibres, but because the properties of different batches of carbon fibre varied somewhat, the strengths and moduli of P1, P3 and P4 were not identical.

Work of fracture values were determined by four-point bend tests, in a floor model Instron, on circumferentially notched rectangular bars as shown in Fig. 1a. This test specimen was originally designed to prevent delamination and thus permit an unambiguous study of energy absorption due to fibre pull-out. It was discovered additionally that when CFRG was tested in this way it broke in a completely controlled manner as shown in Fig. 2a so that the crack speed was determined at all stages of failure by the velocity of the Instron cross-head [5]. This permitted the fracture surface energy to be determined as a function of crack speed by measuring the work of fracture (energy absorbed during fracture divided by twice the specimen cross-section) as a function of cross-head velocity. The same technique has been employed here.

Some Charpy impact energies are also reported for composite P3. These were obtained off a small (2.7J) Hounsfield Charpy machine and corrections were made for energy losses due to toss energies and inertial effects. Similar specimens to the work of fracture experiments were used.

TABLE I The properties of the components of composites P1, P2, GC1 and GC2

	Strength (MN m^{-2})	Young's modulus (GN m^{-2})
Pyrex glass	100	60
Glass-ceramic	100	100
High modulus carbon fibre	1400	390
High strength carbon fibre	2200	250

TABLE II The properties of P1, P2, GC1 and GC2

Material	Microstructural details (vol %)				Mean strengths (MN m^{-2})		
	Volume of fibre V_f	Volume of matrix V_m	Volume of open porosity V_{op}	Volume of closed porosity V_{cp}	Bend strength	Interlaminar shear strength	Mean work of fracture (kJ m^{-2})
P1, Pyrex and high modulus fibre	45.9	52.4	0.6	1.1	459	59	3.1
P2, Pyrex and high strength fibre	48.9	46.0	0.3	4.9	575	71	3.6
GC1, Glass-ceramic and high modulus fibre	49.5	41.6	7.3	1.6	558	32	4.5
GC2, Glass-ceramic and high strength fibre	45.7	40.7	4.7	9.0	574	26	10.3

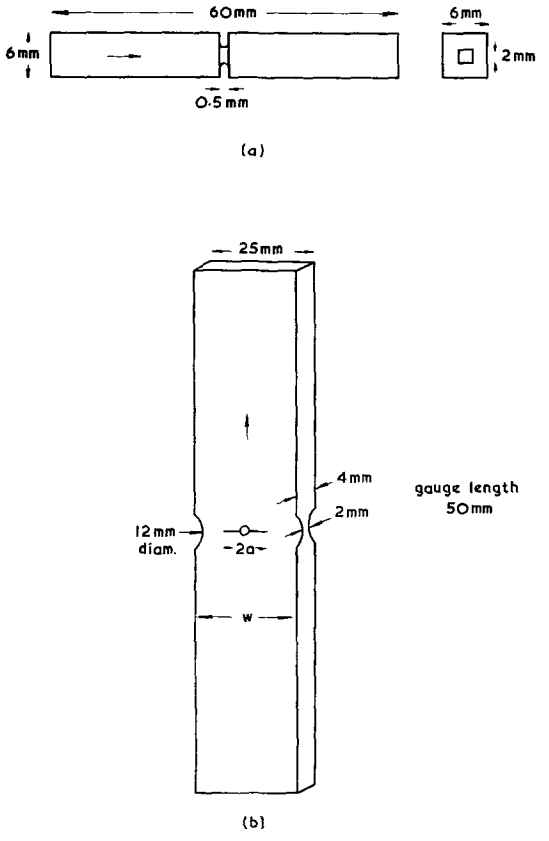

Figure 1 The fracture energy specimens, the arrow indicating fibre direction: (a) work of fracture, (b) centre cracked tensile.

Critical stress intensity factors were determined from tensile measurements on centre-cracked specimens of P4. The specimen dimensions are shown in Fig. 1b. The specimens were radiused at their centres to facilitate propagation

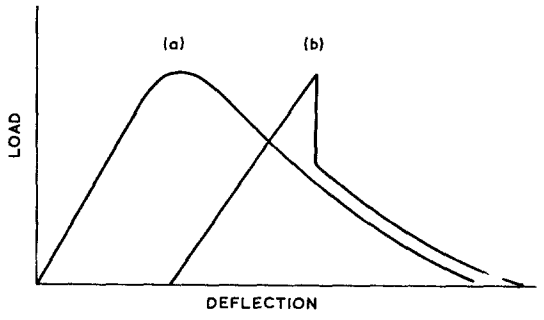

Figure 2 The fracture behaviour of the work of fracture specimens: (a) well controlled, (b) poorly controlled.

of the crack in the correct direction. Cracks were introduced with a fine saw and sharpened with a scalpel.

3. Results

3.1. Effect of material parameters

Fig. 2a shows a completely controlled fracture of the sort that was obtained with circumferentially notched bars of carbon fibre reinforced glass-ceramic. With behaviour of this type, the crack velocity is determined at all stages of fracture by the velocity of the testing machine cross-head. Hence by varying the cross-head velocity it is possible to measure the work of fracture, effectively as a function of crack speed. Fig. 3 shows the dependence of work of fracture of the glass-ceramic composites GC1 and GC2 on cross-head velocity. It can be seen that there is no significant variation of γ_F with cross-head speed. Fig. 2b shows a poorly controlled fracture which was typical of the Pyrex composites P1 and P2 studied in this series of experiments. Where the fractures are not well controlled, the rate of fracture is to some extent

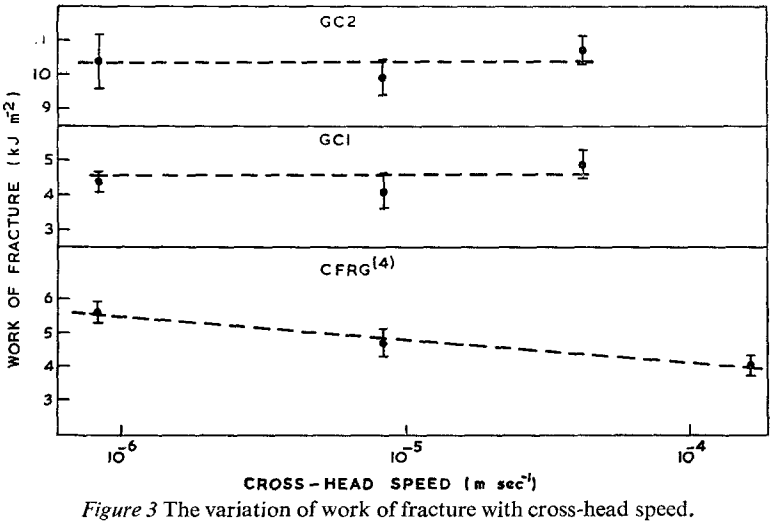

Figure 3 The variation of work of fracture with cross-head speed.

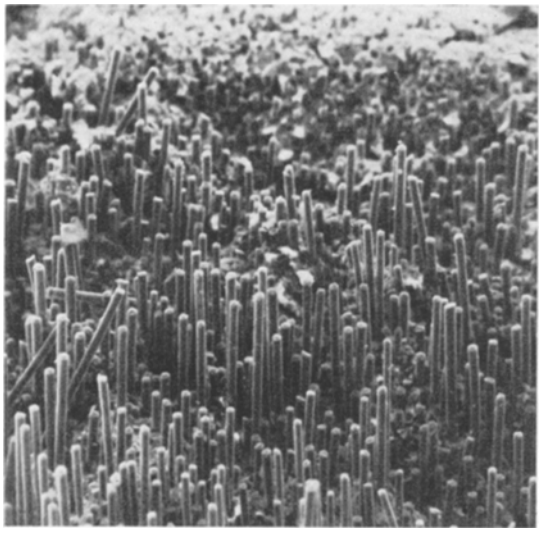

Figure 4 A scanning electron micrograph of a fracture surface showing the protruding fibres (mean diameter 8 μm).

independent of cross-head velocity. It was, therefore, not possible to obtain a relationship between work of fracture and crack speed for P1 and P2. However, Fig. 3 also shows, for comparison with GC1 and GC2, some earlier published data [5] showing the strong dependence of γ_F on cross-head velocity for Pyrex matrix composites which exhibited very well controlled fractures.

Some microstructural measurements have also been made. Fig. 4 shows a typical fracture surface with protruding fibres and Table III shows mean fibre pull-out lengths measured from some of the fracture surfaces of the different specimens. Each mean is the result of several hundred measurements and has a standard error of approximately 5%.

TABLE III Mean fibre lengths protruding from fracture surfaces (μm)

	Material			
Fracture speed	P1	P2	GC1	GC2
Slow	55	53	60	81
Medium	24	36	82	64
Fast	22	35	56	95

3.2. Impact behaviour

The Charpy impact measurements were carried out on material (P3) which displayed a very well controlled fracture in the circumferentially notched work of fracture tests. Data at three low speeds have been published previously [5], but an additional point has been obtained at a higher speed from the Charpy impact tests. Table IV contains the data. The Charpy energy is the mean of seven measurements and the quoted uncertainty is the standard error of the mean. The Charpy impactor struck the specimen at a speed of approximately 2 m sec^{-1} and, on average, was slowed to approximately 0.5 m sec^{-1}. The fracture energy from the Charpy test has been calculated by dividing the energy absorbed by the specimen by twice the fracture surface area. The energy absorbed by the specimen has been calculated from the measured energy lost by the impactor, corrections being made for errors due to the specimen toss energy and inertial effects. It can be seen that the fracture energy does not continue to decrease progressively with increasing fracture rate at higher loading rates.

TABLE IV Comparison of Charpy energy and low speed work of fracture

Test	Fracture speed (m sec^{-1})	Fracture energy (kJ m^{-2})
Work of fracture	8.4×10^{-7}	3.1 ± 0.1
	8.4×10^{-6}	2.7 ± 0.3
	1.7×10^{-4}	2.2 ± 0.2
Charpy impact	2	2.5 ± 0.3

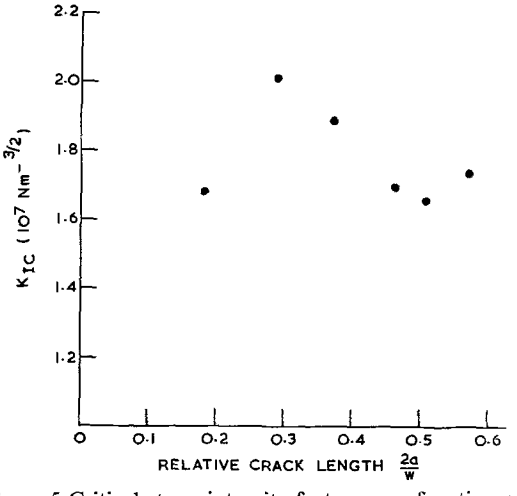

Figure 5 Critical stress intensity factors as a function of crack length.

3.3. Fracture mechanics techniques

Fig. 5 shows critical stress intensity factors (K_{1c}) obtained as a function of crack length ($2a/w$) from centre cracked tensile specimens of P4. All

failed in a planar manner, the crack running perpendicularly to the fibre direction. The K_{1c} values have been calculated from the load at failure using standard formulae [8]. The mean work of fracture of this material obtained with circumferentially notched specimens at a cross-head speed of 10^{-5} m sec^{-1} was 3.5 ± 0.3 kJ m^{-2}.

4. Discussion

4.1. Effect of material parameters on toughness

The results in Table 2 show that: (1) for a given batch of fibre, the glass-ceramic composite yields higher γ_F values than the Pyrex glass composite; (2) for a given matrix material, the high strength fibres yield higher γ_F values than the lower strength, high modulus fibres. These facts can be explained to some extent in terms of the strengths of the fibres and differences in the fibre-matrix interfacial bond.

It is believed that the transfer of stress between fibres and matrix in carbon fibre reinforced glasses is due largely to mechanical keying between fibres and matrix. There is no evidence of chemical bonding and, unlike carbon fibre reinforced resins in which the resin contracts on to the fibre during curing, on cooling CFRG and CFRGC during fabrication, the fibres contract radially away from the matrix. During the hot-pressing of these materials, the pressure is maintained on cooling to about 500° C. Table V shows the thermal expansion coefficients of the matrices and the temperature below which plastic deformation of the matrices effectively stops. Table VI contains thermal expansion coefficients of the fibres, estimated from their structural anisotropy. From these values, the radial contraction of a fibre from its matrix may be easily calculated as 2.4×10^{-8} m for the glass-ceramic and 0.9×10^{-8} m for the Pyrex matrix. The fibres thus contract further from the glass-ceramic matrix than from the Pyrex matrix. This shrinkage reduces the mechanical keying and this would be expected to lead to reduced fibre-matrix interfacial shear strengths which would be reflected in reduced interlaminar shear strengths. This is in fact observed, as Table II shows that the mean interlaminar shear strengths of the two glass-ceramic composites are approximately equal at 32 and 26 MN m^{-2} respectively, as they are for the Pyrex matrix composites at 59 and 71 MN m^{-2}. The interlaminar shear strengths of the glass-ceramic composites are only about one half of those of the Pyrex matrix composites.

TABLE V Temperature properties of the matrices

	Pyrex glass	Glass-ceramic
Minimum stress relaxation temperature (°C)	520	1000
Thermal expansion coefficient (°C^{-1})	3.5	2.0

TABLE VI Estimated thermal expansion coefficients of the fibres

	Radial (°C^{-1})	Axial (°C^{-1})	
		20°C	400°C
High modulus	8×10^{-6}	-1×10^{-6}	0
High strength	8×10^{-6}	-0.5×10^{-6}	0

The work of fracture values of composites of high modulus fibre in Pyrex glass have been shown to arise mainly from the work done in pulling out fibres against restraining interfacial shear stresses]5]. This also appears to be true, at least approximately, for the three other systems studied here. The work of fracture due to pull-out is

$$\gamma_F = \frac{V_f \tau_i l^2_{max}}{6r} \quad (1)$$

on the assumptions that there is a constant restraining shear stress τ_i, and that the pull-out lengths have an equal distribution of lengths from 0 to l_{max}. The maximum length of fibre which can be pulled out of a matrix is related to the critical transfer length, l_c, this being defined as the minimum length of fibre which can be loaded to its fracture stress in the composite. For a hypothetical fibre of constant strength σ_f along its length and radius r, the critical transfer length is

$$l_c = \frac{\sigma_f r}{\tau_i} \quad (2)$$

and

$$l_{max} = \frac{l_c}{2} . \quad (3)$$

In practice, because the strengths of fibres may vary along their lengths, l_c must be regarded as variable, and this results in a non-equal distribution of fibre pull-out lengths. To an approximation, the mean pull-out length $\bar{l}_p$ is

$$\bar{l}_p = \frac{\bar{l}_c}{4} . \quad (4)$$

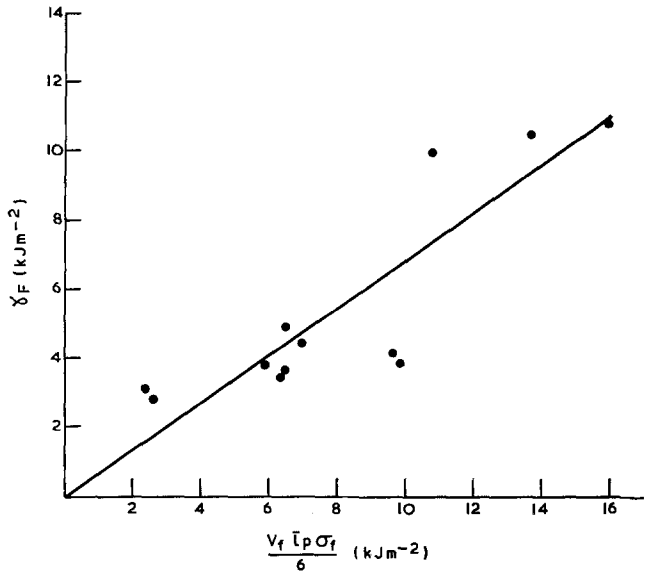

Figure 6 A plot of γ_F versus $V_f\bar{l}_p\sigma_f/6$.

Hence, from Equations 1 to 4

$$\gamma_F = \frac{V_f\sigma_f\bar{l}_p}{6} . \quad (5)$$

Fig. 6 shows γ_F plotted against $(V_f\sigma_f\bar{l}_p/6)$ for materials P1, P2, GC1 and GC2, using the measured strength and pull-out lengths presented in Tables I to III. The agreement with theory is quite reasonable, the points lying on a line which passes through the origin with a slope of about 0.7 instead of the theoretical values of 1.0. Even better agreement can be obtained if it is assumed that the fibres are damaged during composite fabrication and that the appropriate fibre strength to employ in the equation is that calculated from the composite strength via the simple mixtures law. In that case the data lie on a line of slope very much closer to unity. However, this may be fortuitous, as it is not at all certain what is the appropriate fibre strength to use for the small lengths of fibre considered. This, combined with the approximate nature of the theory and the experimental difficulty in measuring l_p precludes any more rigorous conclusions being drawn.

The work of fracture values of these materials can also be related to their other measured properties. From Equations 1, 2 and 3

$$\gamma_F = \frac{V_f r\sigma_f^2}{24\tau_i} . \quad (6)$$

The fibre-matrix interfacial shear stress τ_i is difficult to measure but is certainly related to the interlaminar shear strength of the composite, and one possible method of obtaining this relationship is as follows. It may be assumed that shear failure occurs when the shear stress on a surface through the composite reaches a critical value. Experimentally this surface is a plane through the matrix, which deviates to follow the fibre-matrix interface where it intersects fibres, i.e. sheared fibres are seldom, if ever, observed. The critical shear stress value is $A_i\tau_i + A_m\tau_m$ where A_i is the intersected area of interface, A_m is the area of the plane in the matrix and τ_m is the matrix shear strength. Then for a random distribution of fibres it may be shown [9] that the shear strength of the composite τ_c is

$$\tau_c = x\tau_i + (1 - x)\tau_m \quad (7)$$

where

$$x = \frac{(V_f\pi)^{\frac{1}{2}}}{(V_f\pi)^{\frac{1}{2}} + 1 - 2(V_f/\pi)^{\frac{1}{2}}} .$$

Combining Equations 6 and 7

$$\tau_c = A\frac{V_f\sigma_f^2}{\gamma_F} + B\tau_m$$

where, for composites containing 47 vol % of 4 μm radius fibres, $A = 1.4 \times 10^{-7}$ m and $B = 0.16$.

Fig. 7 shows a plot of τ_c against $V_f\sigma_f^2/\gamma_F$.

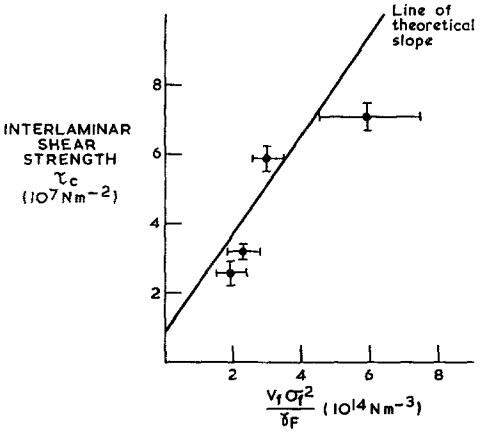

Figure 7 A plot of τ_c versus $V_f\sigma_f^2/\gamma_F$.

Again, quite good agreement is obtained, the straight line, of theoretical slope 1.4×10^{-7} m, intersecting the shear strength axis to imply a very reasonable matrix shear strength of $\sim$ 55 MN m^{-2}. This suggests that the fracture energies of such composites might be predicted from their strength measurements.

4.2. Strain-rate dependence and impact energy

The work of fracture values of the glass-ceramic composites are independent of crack velocity, while it is known that those of the Pyrex matrix composites decrease with increasing crack velocities at low crack velocities. However, the Charpy impact measurements show that the fracture energy of the Pyrex matrix composites does not continue to decrease with increasing crack velocity, instead toughness is retained after an initial decrease.

4.3. Crack initiation and propagation

The tensile tests on the centre-cracked fracture mechanics specimens yielded a mean critical stress intensity factor of 1.78 ($\pm$ 0.06) $\times$ 10^7 MN m$^{-3/2}$. There was no significant trend of K_{1C} varying consistently with crack length, and in each case the cracks propagated perpendicularly to the fibres without deflecting into the low energy direction parallel to them.

In order to calculate G_{1C} values from K_{1C} data off elastically anisotropic materials, it is necessary to use an effective modulus term (E_{eff}) which can be calculated from the elastic modulus matrix of the material [10]

$$G_{1C} = \frac{K_{1C}^2}{E_{eff}} .$$

Using an effective modulus of 55 GN m^{-2}, calculated from the fibre and matrix moduli [5] the calculated value of G_{1C} from fracture mechanics measurements is 5.8 ($\pm$ 0.5) kJ m^{-2}. From work of fracture measurments, $2\gamma_F = 6.9$ ($\pm$ 0.6) kJ m^{-2}. The agreement between these values is much closer than in the earlier work, probably because the crack propagation directions were better controlled, and shows that the large toughness values obtained during work of fracture measurements are also appropriate to fracture initiation.

5. Conclusions

1. The difference in thermal shrinkage between the glass-ceramic and Pyrex matrices results in their composites in differences in the fibre-matrix interfacial shear bond strength τ_i, and hence to differences in the interlaminar shear strengths. The interlaminar shear strength of the Pyrex glass composites is approximately double that of the glass-ceramic composites.

2. The differences in the work of fracture values of Pyrex glass and glass-ceramic reinforced with high modulus and high strength carbon fibres can be explained in terms of the pull-out model.

3. At low strain rates, the work of fracture of CFRG decreases with increasing strain rate, but the work of fracture of CFRGC is strain-rate independent over the same range.

4. The decrease in work of fracture of CFRG with increasing strain rate is not continued indefinitely. The Charpy impact energy at an impact rate of 2 m sec^{-1} is approximately the same as the work of fracture at $\sim 10^{-5}$ m sec^{-1}.

5. Work of fracture and toughness values derived from linear elastic fracture mechanics measurements agree well.

References

1. R. A. J. SAMBELL, D. H. BOWEN and D. C. PHILLIPS, *J. Mater. Sci.* **7** (1972) 663.
2. R. A. J. SAMBELL, A. BRIGGS, D. C. PHILLIPS and D. H. BOWEN, *ibid* **7** (1972) 676.
3. D. C. PHILLIPS, R. A. J. SAMBELL and D. H. BOWEN, *ibid* **7** (1972) 1454.
4. S. R. LEVITT, *ibid* **8** (1973) 793.
5. D. C. PHILLIPS, *ibid* **7** (1972) 1175.
6. H. G. TATTERSALL and G. TAPPIN, *ibid* **1** (1966) 296.
7. R. W. DAVIDGE and G. TAPPIN, *ibid* **3** (1968) 165.

8. A.S.T.M. Special Technical Publication No. 410, "Plane Strain Crack Toughness Testing of High Strength Metallic Materials", 1966.
9. P. HANCOCK and R. C. CUTHBERTSON, *J. Mater. Sci.* **5** (1970) 762.
10. See for example D. C. PHILLIPS and A. S. TETELMAN, *Composites* **3** (1972) 216.

Received 31 May and accepted 21 June 1974.